PHYSICAL REVIEW B **71**, 054505 (2005)

Spin-charge coupling in lightly doped $Nd_{2-x}Ce_xCuO_4$

Shiliang Li and Stephen D. Wilson
Department of Physics and Astronomy, The University of Tennessee, Knoxville, Tennessee 37996-1200, USA

David Mandrus
Condensed Matter Sciences Division, Oak Ridge National Laboratory, Oak Ridge, Tennessee 37831, USA and Department of Physics and Astronomy, The University of Tennessee, Knoxville, Tennessee 37996-1200, USA

Bairu Zhao
Institute of Physics, Chinese Academy of Sciences, P. O. Box 603, Beijing 100080, China

Y. Onose
Spin Superstructure Project, ERATO, Japan Science and Technology, Tsukuba 305-8562, Japan

Y. Tokura
Spin Superstructure Project, ERATO, Japan Science and Technology, Tsukuba 305-8562, Japan Correlated Electron Research Center, Tsukuba 305-8562 Japan and Department of Applied Physics, University of Tokyo, Tokyo 113-8656, Japan

Pengcheng Dai*
Department of Physics and Astronomy, The University of Tennessee, Knoxville, Tennessee 37996-1200, USA and Condensed Matter Sciences Division and Center for Neutron Scattering, Oak Ridge National Laboratory, Oak Ridge, Tennessee 37831, USA

(Received 2 September 2004; revised manuscript received 3 November 2004; published 8 February 2005)

We use neutron scattering to study the influence of a magnetic field on spin structures of Nd_2CuO_4. On cooling from room temperature, Nd_2CuO_4 goes through a series of antiferromagnetic (AF) phase transitions with different noncollinear spin structures. While a *c*-axis aligned magnetic field does not alter the basic zero-field noncollinear spin structures, a field parallel to the CuO_2 plane can transform the noncollinear structure to a collinear one ("spin-flop" transition), induce magnetic disorder along the *c* axis, and cause hysteresis in the AF phase transitions. By comparing these results directly to the magnetoresistance (MR) measurements of $Nd_{1.975}Ce_{0.025}CuO_4$, which has essentially the same AF structures as Nd_2CuO_4, we find that a magnetic-field-induced spin-flop transition, AF phase hysteresis, and spin *c*-axis disorder all affect the transport properties of the material. Our results thus provide direct evidence for the existence of a strong spin-charge coupling in electron-doped copper oxides.

DOI: 10.1103/PhysRevB.71.054505 PACS number(s): 74.25.Fy, 74.72.Jt, 75.25.+z

I. INTRODUCTION

Understanding the role of magnetism in the transport properties and superconductivity of high-transition-temperature (high-T_c) copper oxides remains one of the important unresolved problems in the physics of transition metal oxides.[1] The parent compounds of high-T_c cuprates are antiferromagnetic (AF) ordered Mott insulators composed of two-dimensional (2D) CuO_2 planes. When holes or electrons are doped into these planes, the long-range AF ordered phase is destroyed and the copper oxide materials become metallic and superconducting with persistent short-range AF spin correlations.[2–4] While much work over the past decade has focused on the interplay between magnetism and superconductivity because spin fluctuations may mediate electron pairing for superconductivity,[5,6] understanding the relationship between AF order and transport properties through the metal-insulator transitions (MIT) in these doped copper oxides is interesting in its own right.

For instance, the parent compounds of hole-doped cuprates have collinear AF spin structure, where each Cu^{2+} spin is aligned opposite to its neighbors.[2] For La_2CuO_4 and $La_{2-x}Sr_xCuO_4$ in the lightly doped region, the Cu^{2+} spins in the CuO_2 planes are slightly canted from the direction of the staggered magnetization to form a weak ferromagnetic (FM) moment.[7–9] As a consequence, an applied external magnetic field can manipulate the AF domain structure and induce a large anisotropic magnetoresistance (MR) effect.[10] In the case of the parent compounds of electron-doped materials such as Nd_2CuO_4 and Pr_2CuO_4, the magnetic structures are noncollinear, where spins in adjacent CuO_2 layers are 90 degrees (90°) from each other [Fig. 1(c)], due to the pseudo-dipolar interaction between the rare-earth (Nd^{3+} and Pr^{3+}) and Cu^{2+} ions.[11–13] Application of a magnetic field in the CuO_2 planes will induce a "spin-flop" transition by transforming the noncollinear structure to a collinear one,[14–16] and the critical field ($\mathbf{B}_{SF}$) depends on the direction of the magnetic field with the field along the Cu-Cu ($\mathbf{B}\parallel[\bar{1}10]$) direction

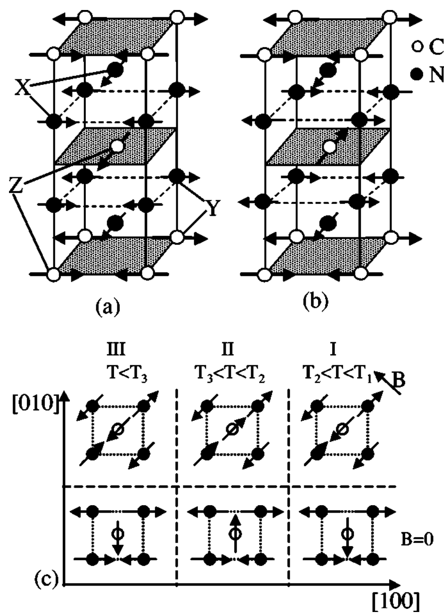

FIG. 1. Nd_2CuO_4 spin structures in (a) type-I/III and (b) type-II noncollinear states, where spins are indicated by the arrows. X, Y, and Z represent the interactions between Nd-Nd, Nd-Cu, and Cu-Cu spins, respectively, as defined by Sachidanandam *et al.* (Ref. 12). (c) The schematic phase diagram of CuO_2 planes in different phases at zero-field (bottom row) and $\mathbf{B}_{SF} \| [1\bar{1}0]$ (top row). Here only Cu spins are shown for clarity. The filled and unfilled circles represent $L=0$ and $1/2$ layers of Cu atoms, respectively. T_1, T_2, and T_3 represent transition temperatures for the three different noncollinear phases at zero field (Ref. 11).

generally having a smaller $\mathbf{B}_{SF}$.[17] A c-axis aligned magnetic field has no effect on the noncollinear spin structure.[18]

Recently, Lavrov *et al.*[19] have reported that an in-plane magnetic field can induce a large MR effect in lightly electron-doped copper oxide $Pr_{1.3-x}La_{0.7}Ce_xCuO_4$ ($x=0.01$). The authors find fourfold-symmetric angular-dependent MR oscillations for $Pr_{1.29}La_{0.7}Ce_{0.01}CuO_4$ in the low-temperature nonmetallic regime. Similar data have also been obtained in nonsuperconducting $Pr_{1.85}Ce_{0.15}CuO_4$ independently.[20] Since $Pr_{1.29}La_{0.7}Ce_{0.01}CuO_4$ has a noncollinear spin structure at low temperatures and the critical fields for spin-flop transition and MR effects are similar, the MR phenomenon in this material has been attributed to the spin structure rearrangement from the noncollinear to the collinear state.[19] For a c-axis aligned magnetic field, the observed negative MR effect in the normal state of several different electron-doped cuprates has been interpreted as a result of two-dimensional weak localization by disorder,[21] Kondo scattering from Cu^{2+} spins in the CuO_2 plane,[22] or spin scattering from field-induced magnetic droplets formed around impurities.[23]

While these recent MR measurements on $Pr_{1.29}La_{0.7}Ce_{0.01}CuO_4$ and $Pr_{1.85}Ce_{0.15}CuO_4$ clearly suggest a close coupling between spin-flop transition and MR effects,[19] the data may also be interpreted as partial rearrangement of magnetic domain walls by magnetic field to allow conductivity of electrons along a preferred direction.[20] In the latter case, the magnetic domain walls are segregated by the doped charge carriers into inhomogeneous patterns, such as stripes.[24] If the transport properties in lightly electron-doped cuprates are indeed determined by spin reorientations and not by stripes, one would expect intimate correlations between the MR effects and spin-flop transitions in other families of electron-doped materials. Since Nd_2CuO_4 exhibits three AF phase transitions with different noncollinear spin structures on cooling from room temperature,[14,15,18] far more complicated than the single AF phase transition found in $Pr_{1.29}La_{0.7}Ce_{0.01}CuO_4$ (Ref. 19) or $Pr_{1.85}Ce_{0.15}CuO_4$,[20] a combined neutron scattering and MR investigation should shed new light on the interplay between spin and charge coupling in the material.

In this paper, we describe our neutron scattering and MR measurements on single crystals of Nd_2CuO_4 and lightly electron-doped $Nd_{1.975}Ce_{0.025}CuO_4$, respectively. For neutron scattering, we choose to study Nd_2CuO_4 because of its complicated AF phase transitions.[14] While previous work showed that a magnetic field applied parallel to the CuO_2 planes transforms the spins from the noncollinear to collinear AF structure,[14,15] there is no systematic work on how the field-induced collinear spin structure affects the zero-field AF phase transitions. We find that application of a $\mathbf{B} \| [1\bar{1}0]$ field can induce c-axis spin disorder and hysteresis in the AF phase transitions. Since lightly electron-doping the insulating Nd_2CuO_4 induces enough charge carriers to allow transport measurements[19] but does not change its basic AF spin structures,[25] we compare the MR effects in $Nd_{1.975}Ce_{0.025}CuO_4$ to the neutron scattering results on Nd_2CuO_4. Surprisingly, we find that the transport properties of $Nd_{1.975}Ce_{0.025}CuO_4$ are very sensitive to the modifications of spin structures in the system. Our results thus provide further evidence for the existence of a strong spin-charge coupling in electron-doped copper oxides. The organization of this paper is as follows. In Sec. II we describe the experimental setup for neutron scattering and transport measurements. Our neutron scattering results are presented in Sec. III while MR transport data are shown in Sec. IV. In Sec. V we compare the neutron scattering and transport data. Finally, Sec. VI summarizes the conclusions of our work.

II. EXPERIMENTAL SETUP

We grew single crystals of Nd_2CuO_4 and $Nd_{1.975}Ce_{0.025}CuO_4$ by the traveling solvent floating-zone method. The samples were grown at a speed of 1 mm/h under 4 atm O_2 pressure in a sealed quartz tube.[26] All the crystals are single domain as confirmed by a polarizing light microscope and Laue x-ray diffraction. The Nd_2CuO_4 single crystals are cylindrical and have dimensions of about 4 mm in diameter and 15 mm in length.

The neutron scattering measurements on Nd_2CuO_4 were performed on the HB-1 and HB-3 triple-axis spectrometers at the high-flux-isotope reactor (HFIR), Oak Ridge National Laboratory (ORNL). We specify the momentum transfer (q_x, q_y, q_z) in units of Å^{-1} as $(H,K,L)=(q_x a/2\pi, q_y b/2\pi, q_z c/2\pi)$ in reciprocal lattice units (rlu). The lattice parameters of the tetragonal unit cells of Nd_2CuO_4 are $a=b=3.944$ Å and $c=12.169$ Å. To prevent the samples from rotating under the influence of a magnetic field, they were

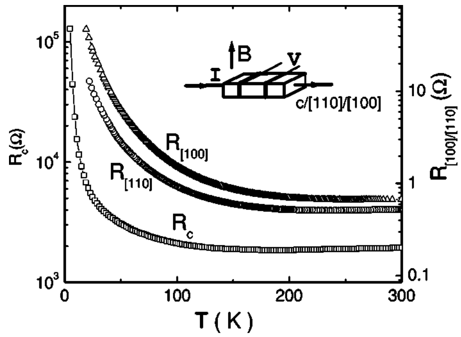

FIG. 2. The temperature dependence of R_c, $R_{[100]}$, and $R_{[110]}$ at zero field, where the subscripts represent the current directions. The resistances in all three directions go up rapidly with decreasing temperature. The inset shows the regular four-points setup. Throughout the measurement, the c axis of the crystal is always along the axis of rotation and the magnetic field rotates within the CuO_2 (ab) plane.

clamped on solid aluminum brackets and placed inside a 7 -T vertical field magnet.[18] For the experiment, we use pyrolytic graphite as the monochromator, analyzer, and filters. The collimations were, proceeding from the reactor to the detector, $48'$-$40'$-sample- $40'$-$120'$ [full width at half maximum (FWHM)], and the final neutron energy was fixed at $E_f = 14.78$ meV. The experiments were performed in the $[H,H,L]$ scattering plane where the applied vertical field is along the $[\bar{1}10]$ direction ($\mathbf{B} \| [\bar{1}10]$) in the CuO_2 plane.

For our transport studies we align and cut one $Nd_{1.975}Ce_{0.025}CuO_4$ single crystal into three rectangular blocks, whose typical size was $3\times1\times0.5\ \mathrm{mm}^3$. Using the regular four-points method, as shown in the inset of Fig. 2, the resistance was measured by the ac-transport option of a commercial 14-T physical property measurement system (PPMS). The ac currents were chosen along the [100], [110], and [001] directions and the corresponding resistance were labeled as $R_{[100]}$, $R_{[110]}$, and R_c, respectively. Since $Nd_{1.975}Ce_{0.025}CuO_4$ has tetragonal crystal structure, the a and b axes are indistinguishable. As a consequence, a magnetic field along the [100] ([110]) direction is equivalent to the [010] ($[\bar{1}10]/[1\bar{1}0]$) direction. Figure 2 shows the temperature dependence of zero-field resistances in the three high symmetry directions. Similar to lightly doped $Pr_{1.29}La_{0.7}Ce_{0.01}CuO_4$,[19] resistances in all directions of $Nd_{1.975}Ce_{0.025}CuO_4$ increase with decreasing temperature and show an insulating behavior at low temperatures. In addition, the resistivity data show no obvious indication of the influence of AF phase transitions. Since $Nd_{1.975}Ce_{0.025}CuO_4$ is only slightly doped away from Nd_2CuO_4, it is reasonable to assume that these two systems have similar spin structures and AF phase transitions.[25]

III. NEUTRON SCATTERING RESULTS

Before describing our results on the influence of an in-plane magnetic field on the magnetic order of Nd_2CuO_4, we briefly review its zero-field spin structures.[14,15] When Nd_2CuO_4 is cooled from room temperature to $T_1 \approx 275$ K, its Cu spins first order into the noncollinear type-I spin structure of Figs. 1(a) and 1(c). On further cooling to $T_2 \approx 75$ K, the Cu spins in the adjacent layer rotate by 180° about the c axis from the type-I phase and reorient the system into type-II phase [Fig. 1(b)]. Finally below $T_3 \approx 30$ K, the Cu spins rotate back to their original direction to form the type-III phase [see Fig. 1(c)].[18] Magnetic structure factors ($|F(1/2,1/2,L)|$) for noncollinear type-I and III phases at $(1/2,1/2,L)$ positions are

$$|F(L=\mathrm{odd})|^2 = 32(\gamma e^2/2mc^2)^2 \times |f_{\mathrm{Cu}}M_{\mathrm{Cu}} + 2\cos(2\pi Lz) f_{\mathrm{Nd}}M_{\mathrm{Nd}}|^2;$$

$$|F(L=\mathrm{even})|^2 = 32(\gamma e^2/2mc^2)^2 \times (2aL/c)^2/[2+(2aL/c)^2] \times |f_{\mathrm{Cu}}M_{\mathrm{Cu}} + 2\cos(2\pi Lz) f_{\mathrm{Nd}}M_{\mathrm{Nd}}|^2. \quad (1)$$

For type-II noncollinear spin structure, we have

$$|F(L=\mathrm{odd})|^2 = 32(\gamma e^2/2mc^2)^2 \times (2aL/c)^2/[2+(2aL/c)^2] \times |f_{\mathrm{Cu}}M_{\mathrm{Cu}} + 2\cos(2\pi Lz) f_{\mathrm{Nd}}M_{\mathrm{Nd}}|^2;$$

$$|F(L=\mathrm{even})|^2 = 32(\gamma e^2/2mc^2)^2 \times |f_{\mathrm{Cu}}M_{\mathrm{Cu}} + 2\cos(2\pi Lz) f_{\mathrm{Nd}}M_{\mathrm{Nd}}|^2; \quad (2)$$

where $\gamma e^2/2mc^2 = 0.2695\times10^{-12}$ cm, $z=0.35$, and f_{Cu}, f_{Nd}, M_{Cu}, and M_{Cu} are magnetic form factors and ordered magnetic moments for Cu and Nd ions, respectively.

From the magnetic structure factor calculations, we find that the intensities of AF Bragg peaks at the $(1/2,1/2,L)$ positions depend sensitively on the detailed spins arrangement. For example, when Nd_2CuO_4 is cooled below the spins reorientation transition temperature T_2 [Fig. 1(c)], intensity of the $(1/2,1/2,1)$ peak decreases while that of $(1/2,1/2,2)$ increases.[11] On further cooling to below T_3, the scattering at these positions recover to their high temperature values [Figs. 3(a) and 3(b)]. Gaussian fits to the data show that the scattering is resolution limited with the FWHM of 0.02 rlu for $(1/2,1/2,1)$ (or $\Delta L = 0.02$ rlu). In principle, one should calculate the coherence length of a Bragg peak from the formula of N-slit grating diffraction.[27] However, the line shape of our observed diffraction peaks is well-described by a Gaussian, equivalent to the N-slit function in the limit of large N. By Fourier transform of the Gaussian peak, we estimate a minimum spin-spin coherence length of ~530 Å using $CL = [4\ln(2)/\pi](c/\Delta L)$.

When a 5-T magnetic field is applied along the $[\bar{1},1,0]$ direction, the noncollinear spin structures at different temperatures are transformed into collinear spin structures [Fig. 1(c)]. In phases I and III, $(1/2,1/2,L=\mathrm{odd})$ peaks vanish while $(1/2,1/2,L=\mathrm{even})$ are enhanced with magnetic structure factors as

$$|F_c(L=\mathrm{even})|^2 = 64(\gamma e^2/2mc^2)^2 \times (2aL/c)^2/[2+(2aL/c)^2] \times |f_{\mathrm{Cu}}M_{\mathrm{Cu}} + 2\cos(2\pi Lz) f_{\mathrm{Nd}}M_{\mathrm{Nd}}|^2. \quad (3)$$

For phase II, $(1/2,1/2,L=\mathrm{even})$ peaks vanish while $(1/2,1/2,L=\mathrm{odd})$ reflections change as

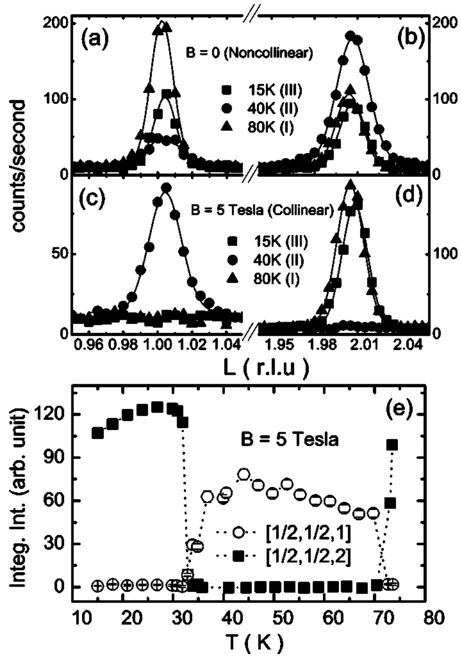

FIG. 3. Typical neutron scattering results around $(1/2,1/2,1)$ and $(1/2,1/2,2)$ Bragg peaks in the (a),(b) $\mathbf{B}=0$ spin noncollinear and (c),(d) $\mathbf{B}=5$ T spin collinear states. We probed the magnetic Bragg peaks at 15, 40, and 80 K in type-III, II, and I phases, respectively. All peaks are fit by Gaussians on sloped backgrounds as shown by the solid lines. (e) The temperature dependence of the integrated intensities at $(1/2,1/2,1)$ and $(1/2,1/2,2)$ positions at $\mathbf{B}=5$ T. The type-III to II and type-II to I collinear phase transitions are around 30 and 70 K, respectively.

$$|F_c(L=\text{odd})|^2 = 64(\gamma e^2/2mc^2)^2 \times |f_{\text{Cu}}M_{\text{Cu}} + 2\cos(2\pi Lz) f_{\text{Nd}}M_{\text{Nd}}|^2. \quad (4)$$

Figures 3(c) and 3(d) confirm that $(1/2,1/2,1)$ is enhanced while $(1/2,1/2,2)$ vanishes after spin-flop transition. Figure 3(e) shows the integrated intensities at the $(1/2,1/2,1)$ and $(1/2,1/2,2)$ positions as a function of increasing temperature after a 5-T magnetic field is applied at 15 K to induce the type-III collinear state [Fig. 1(c)]. From the temperature dependence of their intensities, it is clear that spin-flop transitions occur between the three collinear states at similar temperatures as that of the zero-field AF phase transitions.[18]

To test whether the field-induced type-II collinear spin structure depends on the magnetic field hysteresis, we perform neutron experiments at 40 K in two ways. We first cool the sample at zero-field to 40 K and then increase the $\mathbf{B}\|[\bar{1}10]$ field to 5 T as sketched in the inset of Fig. 4(a) (process **a**). The $[1/2,1/2,L]$ scan from $0.8<L<5.2$ rlu shows resolution-limited peaks around $L=1$, 3, and 5 as shown in Fig. 4(b). Since the $(1/2,1/2,1)$ peak has a Gaussian line shape with FWHM of 0.02 rlu along the L direction, we estimate that the c-axis magnetic coherence length is around 530 Å. Now, if we applied the 5-T field at 15 K and then increased the temperature to 40 K (process **b**), the $(1/2,1/2,L)$ (L=odd) peaks remain but with much different line shape [Fig. 4(c)]. Instead of having resolution-limited

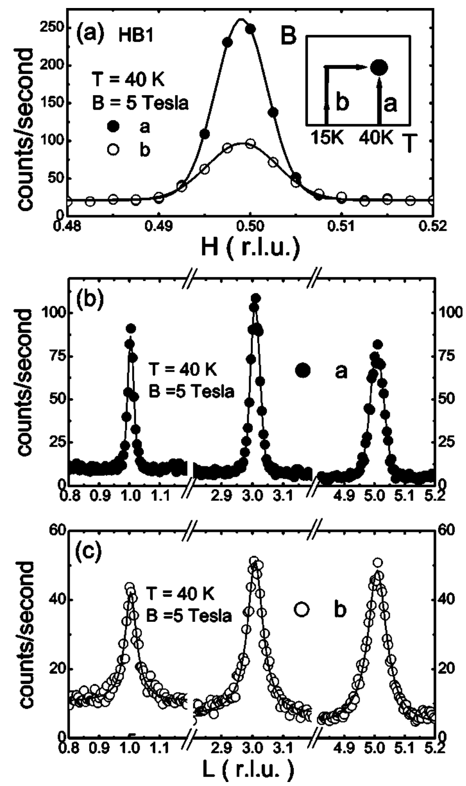

FIG. 4. (a) The in-plane $[H,H,1]$ scans across $(1/2,1/2,1)$ in two different processes at 40 K. The schematic diagrams of processes **a** and **b** are shown in the inset. (b) The long $[1/2,1/2,L]$ scan in process **a**, where L changes from 0.8 to 5.2 rlu. Only three resolution-limited peaks are found around $L=1$, 3, and 5. (c) Same scans as (b), but through process **b**. Note that the L-widths of these peaks become considerably broader. The temperature and field in (b) are identical as that of (c), i.e., $T=40$ K and $\mathbf{B}=5$ T. However, the processes of applying field are different, as shown in the inset of (a). The peaks in (b) and (c) are fitted by Gaussians and Lorentzians, respectively.

Gaussian line shape, the peaks are Lorentzians (the Ornstein-Zernike form) with much broader widths but the same integrated intensities as those in Fig. 4(b). For example, while the FWHM of the $(1/2,1/2,1)$ peak increases to 0.046 rlu from 0.02, its peak intensity also drops by $\sim$50% [Figs. 4(b) and 4(c)]. These observations suggest that the c-axis spin-spin correlation function decays exponentially with a much shorter coherence length [$\sim$84 Å using $1/\kappa$ where κ is half-width at half maximum in Å^{-1} of the Lorentzian in Fig. 4(c)] in process **b**. Since the only difference between the type-III and II collinear states is the 180° spins rotation in adjacent layers [Fig. 1(c)], the short spin-spin coherence length in Fig. 4(c) suggests the presence of a c-axis spin disorder. On the other hand, in-plane scans along the $[H,H,L]$ (L=1, 3, 5) direction only show slight broadening when field is applied at low temperature in process **b** [Fig. 4(a)], thus suggesting most of the spin disorder occurs along the c axis.

To further investigate how hysteresis in application of a magnetic field can affect the spin arrangements in Nd_2CuO_4, we studied its c-axis coherence lengths in all three collinear phases shown in Fig. 1(c). There are three different ways to reach the expected temperature and field of 40 K and 5 T in

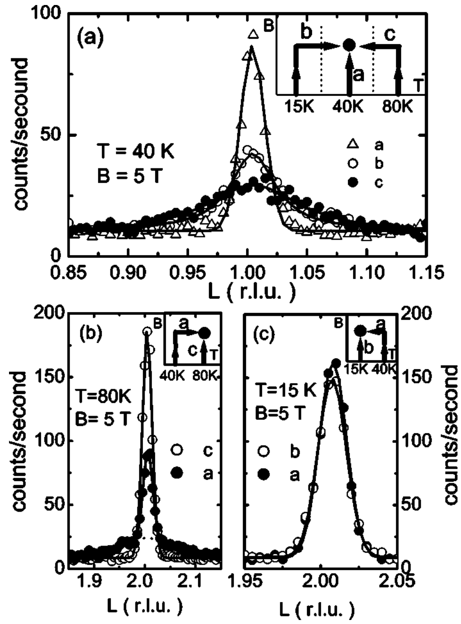

FIG. 5. Magnetic field hysteresis effects on AF spin structures of Nd_2CuO_4 in all three phases. (a) $(1/2,1/2,1)$ Bragg position in phase II and (b) and (c) $(1/2,1/2,2)$ position in phase I and III, respectively. The corresponding processes of field and temperature are shown in the inset of each figure.

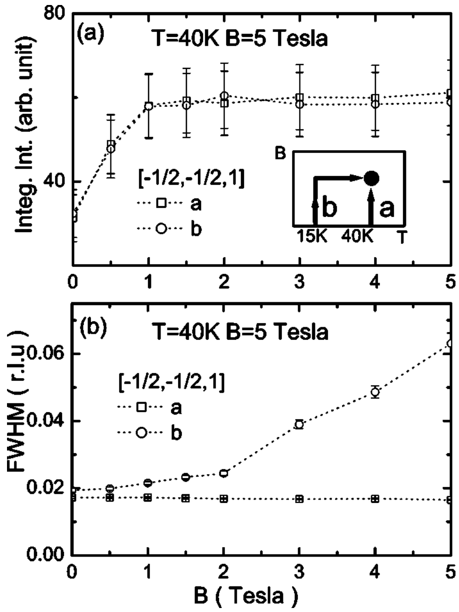

FIG. 6. The field dependence of (a) integrated intensities and (b) FWHMs at the $(1/2,1/2,1)$ position during two different processes shown in the inset of (a). The error bars in (a) are obtained by taking the square root of total summed intensity in L-scans.

the type-II collinear spin phase, which are labeled as **a**, **b**, and **c** in the inset of Fig. 5(a). Processes **a** and **b** are the same as Fig. 4 and process **c** involves getting to 80 K in zero field, applying the 5-T field, and then cooling the sample to 40 K. In other words, the spin system changes from the noncollinear state to the collinear state and remains in type-II collinear spin phase during process **a**, whereas the system undergoes phase transitions from type-III and type-I collinear states to type-II collinear state in processes **b** and **c**, respectively [Fig. 1(c)].

By comparing the $(1/2,1/2,1)$ data of Fig. 4 in processes **a** and **b** with that of **c** in Fig. 5(a), it becomes clear that processes **b** and **c** have considerably broader widths. This means that **b** and **c** processes induce large c-axis spins disorder and the amount of disorder depends on the history of field application. When the system is in type-I phase at 80 K, the collinear spin phase can be induced either by simply applying a field at 80 K [process **c** in the inset of Fig. 5(b)], or by having a type-II collinear phase at 40 K and then increasing the temperature to 80 K [process **a** in the inset of Fig. 5(b)]. Clearly, the $[1/2,1/2,L]$ $(L=2)$ scans in Fig. 5(b) show a resolution-limited Gaussian peak in **c** but a two components line shape with a sharp Gaussian peak on a broad Lorentzian background in process **a**. These results again suggest that magnetic field hysteresis affects mostly the spin arrangements along the c axis. Finally, when temperature is in the type-III collinear phase at 15 K, we find no obvious difference between the two processes in the inset of Fig. 5(c): one of which is applying field at 40 K and then decreasing the temperature to 15 K (process **a**), and the other is applying the field at 15 K directly (process **b**). Therefore spin disorder appears whenever phase transition occurs between two different collinear states except for the transition from type-II to III.

Figure 6 shows the magnetic field dependence of the $(1/2,1/2,1)$ peak at $T=40$ K under different conditions. When a $\mathbf{B}\parallel[1\bar{1}0]$ field is applied from the zero-field noncollinear type-II state at 40 K [process **a** in the inset of Fig. 6(a)], a noncollinear to collinear spin-flop transition occurs around 1 T, and the FWHM of the peak does not change during the process [Figs. 6(a) and 6(b)]. This suggests that the entire AF structure responds to the influence of the applied field. If we warm to 40 K using process **b** shown in the inset of Fig. 6(a), the $(1/2,1/2,1)$ peak has a broad FWHM along the c axis but with the same integrated intensity as process **a**. As a function of decreasing magnetic field at 40 K, the FWHM of $(1/2,1/2,L)$ at $L=1$ decreases continuously until reaching the value of process **a**. This suggests that long-range c-axis spin coherence length is restored in the process.

Because the spin disorder is related to the phase transitions under field, it is natural to ask what happens to the transition itself under different conditions. Here, we use two ways to pass the type-II to type-III phase transition, and label them as processes **a** and **d** in the inset of Fig. 7(a). We carefully monitor the $(1/2,1/2,1)$ peak as the system passing the transition under different conditions. At each measured temperature, we wait 10–15 min to ensure that the peak intensity has no time dependence and the outcome of the experiment is summarized in Fig. 7. Surprisingly, there is a clear hysteresis in the phase transition behavior, i.e., the transition temperature of process **b** is about 2 K higher than that of process **a**.

To understand how this hysteresis occurs, we decreased the temperature following process **b**, i.e., we probe the

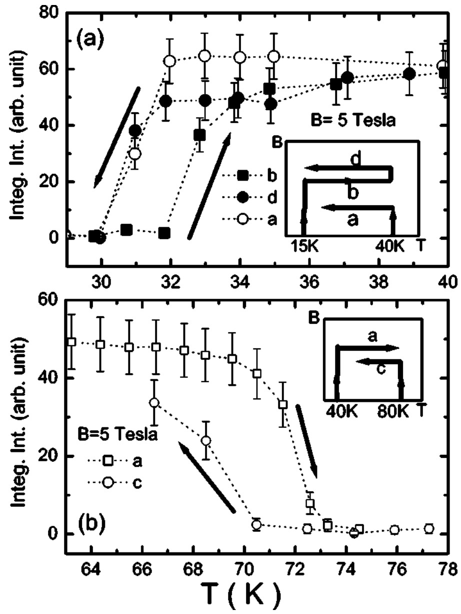

FIG. 7. The integrated intensities of $(1/2,1/2,1)$, which shows temperature hysteresis across the transition (a) between type-II and III phases, and (b) between type-I and II phases. The arrows in the figures indicate the direction of changing temperatures. The insets show the detailed processes of field-temperature hysteresis.

$(1/2,1/2,1)$ peak in process **d** after **b**. Figure 7(a) indicates that the transition temperatures of processes **a** and **d** are identical. While this suggests that spin disorder itself may not induce the lower transition temperature in decreasing temperature processes, the observed hysteresis must be associated with the field-induced collinear spin structures and their free-energy differences in different phases. Similar hysteresis behavior can also be found for the transition between collinear type-II and I phases [Fig. 7(b)]. In this case, the integrated intensities of $(1/2,1/2,1)$ during process **c** are much smaller than those during process **a** below 70 K, while the intensities of $(1/2,1/2,2)$ remain zero thus ruling out a possible mixture of the two phases.

In previous work on Pr_2CuO_4,[28] which has a noncollinear type-I/III spin structure [Fig. 1(a)],[16] diffuse scattering associated with interplane short-range order was observed above the spin-flop transition critical field (3.1 T) around the forbidden AF position $(1/2,1/2,1)$ at $T=1.5$ K. Since similar diffuse scattering was not observed around $(1/2,1/2,2)$, the authors suggest that the diffuse scattering arises from the persistent midrange interplane correlations.[28] For Nd_2CuO_4, we find no evidence for similar short-range order spin order at $(1/2,1/2,1)$ (Figs. 2–5). Instead, we find clear evidence for field-induced AF phase transition hysteresis and spin disorder. If the spin degree of freedom is strongly coupled to the charge carriers, one would expect to observe changes in electrical transport properties uniquely associated with field-induced spin disorder and hysteresis in these materials. By performing systematic MR measurements in lightly doped $Nd_{1.975}Ce_{0.025}CuO_4$, which have essentially the same AF structure as Nd_2CuO_4 but with enough charge carriers for resistance measurements, we can directly compare the transport data with neutron scattering results. The following section will describe such a comparison.

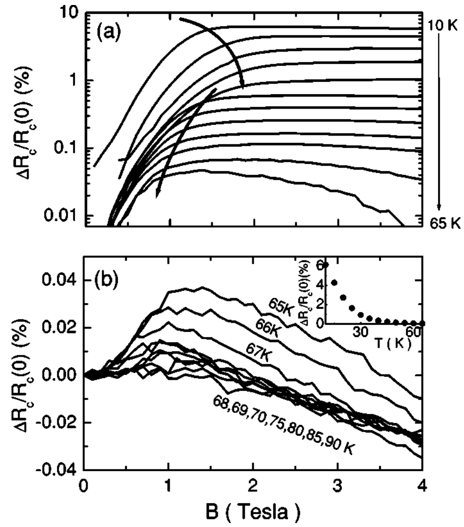

FIG. 8. $\Delta R_c/R_c(0)$ as a function of increasing magnetic field at different temperatures around (a) 30 K and (b) 70 K. Note that these temperatures are close to T_3 and T_2, respectively. The applied magnetic field is in the CuO_2 *ab*-plane along the $[\bar{1}10]$ direction. The arrows in (a) indicate the temperature dependence of $\mathbf{B}_{SF}$. The inset in (b) plots the maximum of $\Delta R_c/R_c(0)$ as a function of increasing temperature. It shows $1/T$ behavior. Note that the vertical axes are log scale in (a) and linear scale in (b).

IV. MAGNETORESISTANCE RESULTS

In the work of Lavrov and co-workers on $Pr_{1.29}La_{0.7}Ce_{0.01}CuO_4$,[19] the similarities between the critical field for the spin-flop transition and the rapid increase of MR have been taken as evidence for spin-charge coupling. Because there exists three spin phases in Nd_2CuO_4 whereas only one in $Pr_{1.29}La_{0.7}Ce_{0.01}CuO_4$, one would expect some new phenomena related to those phases and the transitions between them. Figure 8 shows the *c*-axis MR effect $\Delta R_c/R_c(0)$ of $Nd_{1.975}Ce_{0.025}CuO_4$ at different temperatures. As a function of increasing field along the $[\bar{1}10]$ direction, $R_c/R_c(0)$ initially increases quickly but then descends slightly. The increase in the critical field for spin-flop transition, $\mathbf{B}_{SF}$, with increasing temperature for T below 30 K is consistent with earlier neutron scattering experiments on Nd_2CuO_4.[14] The increase of $\mathbf{B}_{SF}$ with increasing temperature ends above $T_3=31$ K, where the type-III to type-II spin-flop transition occurs [Fig. 8(a)]. Compared with the results on $Pr_{1.29}La_{0.7}Ce_{0.01}CuO_4$,[19] the data suggest that the changes in MR effect originate from the differences of $\mathbf{B}_{SF}$ in three different spin phases. Below 30 K, $\mathbf{B}_{SF}$ increases slightly with increasing temperature. It then decreases with increasing temperature beyond 30 K. Finally, when the system changes to type-I phase above 67 K, the sharp increase of $R_c/R_c(0)$ at low fields almost disappears, and all $\Delta R_c/R_c(0)$ data nearly fall into one curve [Fig. 8(b)]. Similar phenomena are also found for $R_{[110]}/R_{[110]}(0)$ and $R_{[100]}/R_{[100]}(0)$. The temperature dependence of the maximum of $\Delta R_c/R_c(0)$ is shown in the inset of Fig. 8(b), which can be fit by the $1/T$ function similar to low temperature intensity changes in Nd_2CuO_4 (Ref. 18) and $Nd_{1.85}Ce_{0.15}CuO_4$.[29]

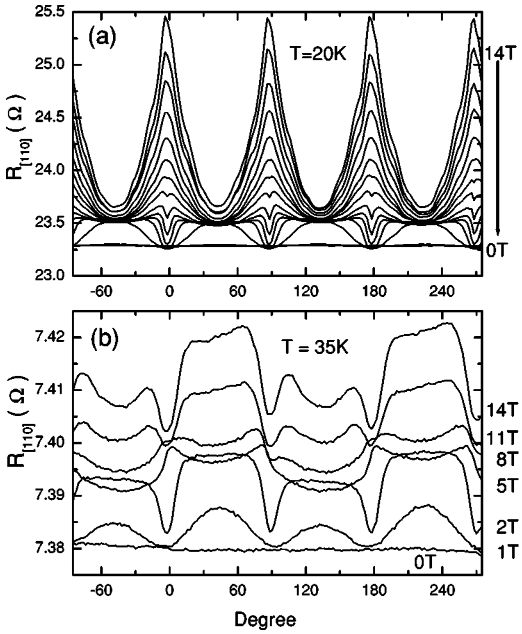

FIG. 9. Angular dependence of $R_{[110]}$ at (a) $T=20$ K in type-III phase and (b) $T=35$ K in type-II phase, where [110] indicates the current direction. The horizontal axes represent the angle (in degrees) between the magnetic field and the *a* or *b* axis which cannot be distinguished for the tetragonal system. Note that data in (a) at 1 T show a nonobservable MR effect while there are clear MR effects at 1 T in (b).

In previous work, a fourfold angular oscillation in MR effect has been identified in $Pr_{1.29}La_{0.7}Ce_{0.01}CuO_4$ (Ref. 19) and $Pr_{1.85}Ce_{0.15}CuO_4$ (Ref. 20) for an applied magnetic field in the CuO_2 plane. For lightly doped $Nd_{1.975}Ce_{0.025}CuO_4$, we expect to observe similar fourfold oscillation behavior. In addition, we hope to determine whether transitions across different spin phases affect the MR. To study the angular dependence of resistance, we rotated the sample with respect to the *c* axis which remained perpendicular to the magnetic field, i.e., the field rotated within the *ab*-plane. The rotation angle is defined to be zero when $\mathbf{B}\parallel[100]/[010]$. As shown in Fig. 9(a), a fourfold feature in $R_{[110]}$ similar to the earlier results is found as a function of the rotation angle. While $R_{[110]}$ along the $[110]/[1\bar{1}0]$ direction is much higher than that along the [100]/[010] direction at low fields, the situation reverses itself at high fields.

Assuming a strong spin-charge coupling, one can understand the microscopic process of the MR effect as follows. When an in-plane magnetic field is applied along the $[110]/[1\bar{1}0]$ direction, spins in the type-III noncollinear structure of Fig. 1(c) rotate continuously to form the collinear structure perpendicular to the field.[14] While these diagonal (Cu-Cu) directions are easy axes in the collinear spin structure with relatively small $\mathbf{B}_{SF}[1\bar{1}0]$, a perfectly aligned field along the [100]/[010] direction induces a first-order spin-flop transition with a much larger critical field $\mathbf{B}_{SF}[100]$.[17] For a magnetic field in the intermediate directions, it first induces a transition into the collinear state and then smoothly rotates the spins to positions perpendicular to the field.[17,19] If an applied field is less than 1 T, there is no spin-flop transition at any field orientation and thus no MR effect, consistent with Figs. 8(a) and 9(a). When an applied field ($2\text{ T}\leqslant\mathbf{B}\leqslant 6\text{ T}$) is larger than $\mathbf{B}_{SF}[1\bar{1}0]$ but smaller than $\mathbf{B}_{SF}[100]$, one would expect to observe a spin-flop transition, and therefore the MR effect, for fields along the $[110]/[1\bar{1}0]$ direction but not along the [100]/[010] direction. This is exactly what we find in Fig. 9(a). Finally for $\mathbf{B}\geqslant\mathbf{B}_{SF}[100]$, the aligned collinear spins will simply follow the rotation of the field in all directions. Here the magnitude of the MR effect for $\mathbf{B}\parallel[100]/[010]$ is larger than that for $\mathbf{B}\parallel[110]/[1\bar{1}0]$, therefore causing a new fourfold MR oscillation with 90° angles to shift from that in $\mathbf{B}_{SF}[1\bar{1}0]\leqslant\mathbf{B}\leqslant\mathbf{B}_{SF}[100]$.

As the temperature of the system is increased to 35 K in the type-II phase, the magnitude of $\mathbf{B}_{SF}[1\bar{1}0]$ becomes smaller than that at 20 K.[14,15,19] This explains the observed fourfold MR oscillations in Fig. 9(b) at 1 T, while similar oscillations are only seen for fields above 2 T at 20 K [Fig. 9(a)]. On increasing the applied field from 1 T, the oscillations change from a sinusoidal shape to a flattish (or concave) top but the symmetry of the oscillations as a function of rotational angle remains even up to the maximum field of 14 T. The data are clearly different from that at 20 K for fields above 6 T, where MR effects are maximal along the [100]/[010] directions for $\mathbf{B}\geqslant 6$ T. To consistently interpret the MR data of Figs. 9(a) and 9(b), we speculate that $\mathbf{B}_{SF}[100]$ is larger than the maximum applied field of 14 T around 30 K. While this scenario is difficult to prove because neutron experiments in the $\mathbf{B}\parallel[100]/[010]$ geometry have not yet been carried out at this temperature,[17] a large ($\geqslant$4.5 meV) in-plane spin-wave gap associated with the Nd^{3+}-Cu^{2+} interactions has been reported in the type-II phase of Nd_2CuO_4.[30] If closing such a spin-wave gap is required to induce the spin-flop transition in the $\mathbf{B}\parallel[100]/[010]$ geometry, the critical field necessary to produce Zeeman energy larger than 4.5 meV will exceed 14 T assuming only Cu^{2+} contributions [see Eq. (2)]. Alternatively, one might imagine that the bigger low-temperature MR effect in the $\mathbf{B}\parallel[100]/[010]$ direction is somehow related to the larger Nd^{3+} moments and/or the first order nature of the spin-flop transition in this direction.[19,20] While how MR is affected by the Nd^{3+}-Cu^{2+} coupling is unknown, a small misalignment of the sample with respect to the magnet around [100]/[010] directions can affect dramatically the observed MR. Such misalignment may also explain the slightly different MR values at 45° and 135° in Fig. 9(b). We note that similar, but less obvious, behavior is also present in Fig. 9(a) and in previously reported MR data.[19,20]

Figure 10(a) shows the angular dependence of $R_{[100]}$ at 20 K and 10 T. While $R_{[100]}$ has fourfold oscillations similar to that of $R_{[110]}$ at the same temperature [Fig. 9(a)], the MR differences between 45° and 135° are more obvious. With increasing temperature, the fourfold oscillations are replaced by a square-wavelike feature [Fig. 10(b)] similar to Fig. 9(b). Note that our neutron scattering revealed a clear hysteresis through the type-III to type-II collinear phase transition [Fig.

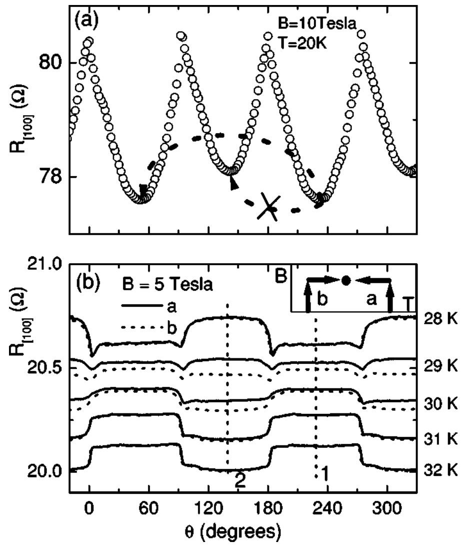

FIG. 10. (a) Angular dependence of $R_{[100]}$ at 20 K and 10 T. While we still observe the fourfold feature, the MR effects do not have the expected 90° symmetry. Although the effect could be an intrinsic property of the material, we speculate that this is due to the small misalignment of the sample with respect to the applied field. (b) Hysteresis behavior of $R_{[100]}$ around the transition between the type-II and III phases at 5 T. At each measured temperature, a constant has been subtracted from the resistance values in processes **a** and **b** for clarity. The solid and dotted lines represent increasing (**b**) and decreasing (**a**) temperatures, respectively, as shown in the inset.

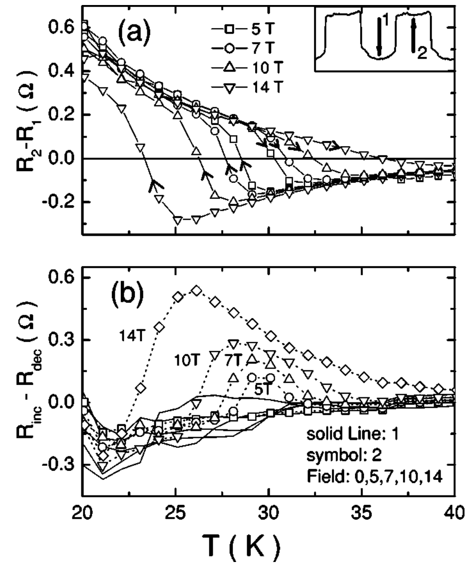

FIG. 11. (a) R_2-R_1 during increasing and decreasing temperature processes, as shown by the arrows. The positions 1 and 2 are defined in the inset of (a). With increasing field, the widths of hysteresis become larger. (b) $R_{inc}-R_{dec}$, the differences between increasing and decreasing temperature processes at positions 1 and 2 are plotted by lines and symbols, respectively.

7(a)]. To see if MR follows such hysteresis, we performed careful measurements on field-warming and cooling as processes **b** and **a**, respectively [see the inset of Fig. 10(b)]. The outcome in Fig. 10(b) shows clear hysteresis across the type-III to type-II transition, consistent with the neutron scattering results of Fig. 7. In addition, we find that the relative value of $R_{[100]}$ shifts 90° across the transition, suggesting that the MR effects are sensitive to the differences in the type-III and type-II collinear spin structures [Fig. 1(c)]. If we define the resistance at 135° position as R_2 and 225° as R_1, R_2 is larger than R_1 in the type-III collinear phase while the reverse is true in the type-II collinear phase.

Using the resistance difference between positions 1 and 2, we probe the phase transition between type-III and type-II collinear states in great detail. If there is no field-induced hysteresis, R_2-R_1 should be the same for either warming or cooling. Figure 11(a) indicates that this is not the case. On warming, the type-III collinear to type-II collinear transition temperature increases with increasing field. On the contrary, the type-II to III transition temperature decreases with increasing field on cooling. As a consequence, the width of the hysteresis increases with increasing field and can be as large as ~15 K at 14 T [Fig. 11(a)]. At 5 T, the width of the hysteresis is about 2 to 3 K, completely consistent with the neutron scattering results of Fig. 7. Figure 11(b) shows the differences in resistance at positions 1 and 2 between increasing and decreasing temperature processes for various applied fields. The results also suggest an increasing hysteresis in the phase transition with increasing magnetic fields, consistent with Fig. 11(a).

Finally, we describe the transport measurements associated with the *c*-axis disorder seen by neutron scattering. Following the same processes as the inset in Fig. 7(a), we have measured the resistance of $Nd_{1.975}Ce_{0.025}CuO_4$ in three different current directions, $R_{[100]}$, $R_{[110]}$, and R_c. For the in-plane resistances, we find no distinguishable difference between $R_{[100]}$ and $R_{[110]}$ after waiting 1 h for each measurement. The results of $R_{[100]}$ at 34 K and 5 T in Fig. 12 show overlapping curves for processes of **a**, **b**, and **d**. On the other hand, R_c displays clear distinctions among the varying processes as shown in Fig. 12. Since the resulting differences in $R_{[100]}$ for processes **a**, **b**, and **d** are less than 5×10^{-5}, we

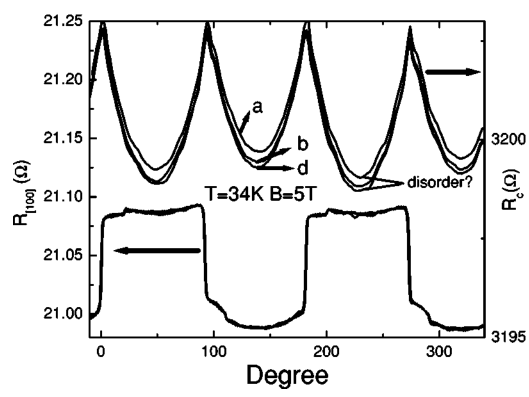

FIG. 12. Angular dependence of $R_{[100]}$ and R_c at 34 K and 5 T through processes **a**, **b**, and **d** similar to that defined in Fig. 7(a), except in this case the final temperature was fixed at 34 K. Process **a** does not cross the phase transition temperature, and therefore does not exhibit disorder. Processes **b** and **d** have spin disorder. While clear differences are seen in R_c, there are no observable differences in $R_{[100]}$ for these different processes.

can safely conclude that the observed deviations in R_c among these processes are intrinsic and may originate from the spin disorder along the c axis. More work is needed to understand the precise relationship between spin disorder and charge transport properties.

V. DISCUSSION

Until now, the most successful theory to understand the spin properties of Nd_2CuO_4 is based on pseudodipolar interaction (PDI) originally proposed by Van Vleck in 1937,

$$V_{pd} = \frac{1}{2}\sum_{\ell\ell'} V(\mathbf{R}_{\ell\ell'})(\mathbf{S}_{\ell'}\hat{\mathbf{R}}_{\ell\ell'})(\mathbf{S}_{\ell}\hat{\mathbf{R}}_{\ell\ell'}), \tag{5}$$

where ℓ and ℓ' denote the lattice sites and the function $V(R)$ decreases faster than R^{-3} as $R\to\infty$. To explain the reorientation of the spin structure, Sachidanandam *et al.*[12] considered three major interplane interactions between Nd-Nd, Nd-Cu, and Cu-Cu, labeled as X, Y, and Z, respectively, in Fig. 1(a). The interactions X and Z tend to generate the type-III or I spin structures, while Y prefers type-II phase. The interactions between spins are proportional to their local susceptibilities (m). Since m_{Nd} is proportional to $1/T$ (Ref. 12) and m_{Cu} varies little below 40 K,[11] $X\propto 1/T^2$, $Y\propto 1/T$, and $Z \approx \mathrm{const}$. With decreasing temperature, Cu-Cu (Z) interactions initially turn on below T_1 and Nd_2CuO_4 orders antiferromagnetically with the type-I spin structure [Fig. 1(a)]. On cooling to intermediate temperature T_2, Nd-Cu (Y) interactions become important and the system transforms to the type-II noncollinear spin structure. Finally below T_3, Nd -Nd (X) interactions dominate and induce the type-III noncollinear spin structure (Fig. 1).

The noncollinear spin structures of Nd_2CuO_4 have a small spin-wave anisotropy gap Δ_0 at zero field.[13] When an in-plane field is applied, the Zeeman energy shifts the spin-wave dispersion and closes the anisotropy energy gap, resulting in a transition from noncollinear to collinear spin-flop phase. Petitgrand *et al.*[13] have given the critical field of spin-flop transition when the field is along the $[\bar{1}10]$ direction,

$$B_{SF}[\bar{1}10] = \frac{\Delta_0}{gm\mu_B}, \tag{6}$$

where Δ_0 is the in-plane spin-wave gap at zero field, g is Landau factor, m the effective moment, and μ_B the Bohr magneton. This equation has been successfully used to explain the temperature dependence of $\mathbf{B}_{SF}[\bar{1}10]$ for Pr_2CuO_4.[16] For Nd_2CuO_4, the in-plane Cu spin-wave gap has a $1/T$ dependence and the out-of-plane gap is essentially temperature independent.[31] In addition, Nd spin waves exhibit anisotropic gaps at low temperatures.[32] Since an applied field of a few Tesla in the CuO_2 will not change the large (>5 meV) Cu spin-wave gap in type-III phase below 30 K,[30] the spin-flop transition there is most likely induced by closing the Nd spin-wave gap.

The existence of a spin-charge coupling has been suggested in lightly electron-doped $Pr_{1.29}La_{0.7}Ce_{0.01}CuO_4$, but a detailed microscopic understanding of how such coupling occurs is still lacking.[19] If the itinerant electrons are coupled to the localized spins directly, one would expect to observe their signatures in the zero-field resistance when $Pr_{1.29}La_{0.7}Ce_{0.01}CuO_4$ and $Pr_{1.85}Ce_{0.15}CuO_4$ order antiferromagnetically,[19,20] and when different noncollinear spin phase transitions occur in $Nd_{1.975}Ce_{0.025}CuO_4$ (Fig. 2). However, AF order appears to have no dramatic effects on zero-field resistance. Instead, the maximum of $\Delta R_c/R_c(0)$ in $Nd_{1.975}Ce_{0.025}CuO_4$ shows a $1/T$ temperature dependence [inset of Fig. 8(b)], very similar to the $1/T$ temperature dependence of the Nd moment in various Nd-containing $Nd_{2-x}Ce_xCuO_4$ compounds.[11,14,15,18,29] This strongly suggests that the observed MR effects in $Nd_{1.975}Ce_{0.025}CuO_4$ and other electron-doped materials are somehow related to the rare earth (Nd, Pr) moments and/or Nd(Pr)-Cu coupling. This picture may also explain why, when the dominant spin-spin interactions are from Cu-Cu with negligible Nd moments in the type-I collinear phase ($T>68$ K), the weak MR data are essentially temperature independent and collapse onto a single curve [Fig. 8(b)].

To compare our results with hole-doped materials, we note that large anisotropic MR effects have already been reported for lightly doped $La_{2-x}Sr_xCuO_4$ (Ref. 10) and $YBa_2Cu_3O_{6+x}$.[33,34] These results have been interpreted as due to the influence of an applied magnetic field on stripes,[10,24,33] spin-orbital coupling,[35] redistribution of magnetoelastic antiferromagnetic domains,[36] or canted AF spin structures.[37] At present, there is no consensus on a microscopic picture for the MR effects in hole-doped copper oxides and more work is needed to test the predictions of different models. However, regardless of the details for each model, what is clear is that transport properties of electron- or hole-doped copper oxides are closely related to the AF order in these materials.

VI. CONCLUSIONS

In summary, we have shown that the spin-flop transition from a noncollinear to collinear state in a lightly electron-doped copper oxide affects both the in-plane and out-of-plane MR. The application of an in-plane magnetic field can induce c-axis spin disorder and hysteresis in the AF phase transitions. By comparing neutron scattering results of Nd_2CuO_4 with the MR effects in $Nd_{1.975}Ce_{0.025}CuO_4$, we show that the transport properties of these materials are very sensitive to the subtle changes in the spin structures. Our results thus provide further evidence for the existence of a strong spin-charge coupling in both electron and hole doped copper oxides.

ACKNOWLEDGMENTS

We would like thank Yoichi Ando and Hai-hu Wen for helpful discussions. This work is supported by the U.S. NSF DMR-0139882, DOE No. DE-AC05-00OR22725 with UT/Battelle, LLC., and by NSF of China under Contract No. 10128408.

*Electronic address: daip@ornl.gov

[1] M. Imada, A. Fujimori, and Y. Tokura, Rev. Mod. Phys. **70**, 1039 (1998).
[2] M. A. Kastner, R. J. Birgeneau, G. Shirane, and Y. Endoh, Rev. Mod. Phys. **70**, 897 (1998).
[3] P. Dai, H. A. Mook, R. D. Hunt, and F. Doğan, Phys. Rev. B **63**, 054525 (2001).
[4] C. Stock, W. J. L. Buyers, R. Liang, D. Peets, Z. Tun, D. Bonn, W. N. Hardy, and R. J. Birgeneau, Phys. Rev. B **69**, 014502 (2004).
[5] S. M. Hayden, H. A. Mook, P. Dai, T. G. Perring, and F. Doğan, Nature (London) **429**, 531 (2004).
[6] J. M. Tranquada, H. Woo, T. G. Perring, H. Goka, G. D. Gu, G. Xu, M. Fujita, and K. Yamada, Nature (London) **429**, 534 (2004).
[7] T. Thio, T. R. Thurston, N. W. Preyer, P. J. Picone, M. A. Kastner, H. P. Jenssen, D. R. Gabbe, C. Y. Chen, R. J. Birgeneau, and A. Aharony, Phys. Rev. B **38**, 905 (1988).
[8] T. Thio, C. Y. Chen, B. S. Freer, D. R. Gabbe, H. P. Jenssen, M. A. Kastner, P. J. Picone, N. W. Preyer, and R. J. Birgeneau, Phys. Rev. B **41**, 231 (1988).
[9] A. N. Lavrov, Y. Ando, S. Komiya, and I. Tsukada, Phys. Rev. Lett. **87**, 017007 (2001).
[10] Y. Ando, A. N. Lavrov, and S. Komiya, Phys. Rev. Lett. **90**, 247003 (2003).
[11] J. W. Lynn and S. Skanthakumar, *Handbook on the Physics and Chemistry of Rare Earths, Vol. 31* (Elsevier Science, New York, 2001), p. 315.
[12] R. Sachidanandam, T. Yildirim, A. B. Harris, A. Aharony, and O. Entin-Wohlman, Phys. Rev. B **56**, 260 (1997).
[13] D. Petitgrand, S. V. Maleyev, Ph. Bourges, and A. S. Ivanov, Phys. Rev. B **59**, 1079 (1999).
[14] S. Skanthakumar, J. W. Lynn, J. L. Peng, and Z. Y. Li, J. Appl. Phys. **73**, 6326 (1993).
[15] S. Skanthakumar, J. W. Lynn, J. L. Peng, and Z. Y. Li, Phys. Rev. B **47**, 6173 (1993).
[16] I. W. Sumarlin, J. W. Lynn, T. Chattopadhyay, S. N. Barilo, D. I. Zhigunov, and J. L. Peng, Phys. Rev. B **51**, 5824 (1995).
[17] V. P. Plakhty, S. V. Maleyev, S. V. Gavrilov, F. Bourdarot, S. Pouget, and S. N. Barilo, Europhys. Lett. **61**, 534 (2003).
[18] M. Matsuura, P. Dai, H. J. Kang, J. W. Lynn, D. N. Argyriou, K. Prokes, Y. Onose, and Y. Tokura, Phys. Rev. B **68**, 144503 (2003).
[19] A. N. Lavrov, H. J. Kang, Y. Kurita, T. Suzuki, S. Komiya, J. W. Lynn, S.-H. Lee, P. Dai, and Y. Ando, Phys. Rev. Lett. **92**, 227003 (2004).
[20] P. Fournier, M.-E. Gosselin, S. Savard, J. Renaud, I. Hetel, P. Richard, and G. Riou, Phys. Rev. B **69**, 220501 (2004).
[21] P. Fournier, J. Higgins, H. Balci, E. Maisier, C. J. Lobb, and R. L. Greene, Phys. Rev. B **62**, R11 993 (2000).
[22] T. Sekitani, M. Naito, and N. Miura, Phys. Rev. B **67**, 174503 (2003).
[23] Y. Dagan, A. Biswas, M. C. Barr, W. M. Fisher, and R. L. Green, cond-mat/0408490 .
[24] S. A. Kivelson, I. P. Bindloss, E. Fradkin, V. Oganesyan, J. M. Tranquada, A. Kapitulnik, and C. Howald, Rev. Mod. Phys. **75**, 1201 (2003).
[25] K. Yamada, K. Kurahashi, Y. Endoh, R. J. Birgeneau, and G. Shirane, J. Phys. Chem. Solids **60**, 1025 (1999).
[26] Y. Onose, Y. Taguchi, T. Ishikawa, S. Shinomori, K. Ishizaka, and Y. Tokura, Phys. Rev. Lett. **82**, 5120 (1999).
[27] B. E. Warren, *X-Ray Diffraction* (Dover, New York, 1990).
[28] D. Petigrand, A. S. Ivanov, and S. V. Maleyev, Appl. Phys. A: Mater. Sci. Process. **74**, S853 (2002).
[29] H. J. Kang, P. Dai, J. W. Lynn, M. Matsuura, J. R. Thompson, S. C. Zhang, D. N. Argyriou, Y. Onose, and Y. Tokura, Nature (London) **423**, 522 (2003).
[30] P. Bourges, A. S. Ivanov, D. Petitgrand, J. Rossat-Mignod, and L. Boudarene, Physica B **186–188**, 925 (1993).
[31] A. S. Ivanov, Ph. Bourges, D. Petitgrand, and J. Rossat-Mignod, Physica B **213–214**, 60 (1995).
[32] N. M. Pyka, M. d'Astuto, A. Metz, A. S. Ivanov, M. Loewenhaupt, H. Casalta, D. Petitgrand, and P. Bourges, Phys. Rev. B **61**, 14 311 (2000).
[33] Y. Ando, A. N. Lavrov, and K. Segawa, Phys. Rev. Lett. **83**, 2813 (1999).
[34] E. Cimpoiasu, V. Sandu, C. C. Almasan, A. P. Paulikas, and B. W. Veal, Phys. Rev. B **65**, 144505 (2002).
[35] A. S. Moskvin and Yu. D. Panov, Solid State Commun. **122**, 253 (2002).
[36] E. V. Gomonaj and V. M. Loktev, Phys. Rev. B **64**, 064406 (2001).
[37] V. Juricic, L. Benfatto, A. O. Caldeira, and C. Morais Smith, Phys. Rev. Lett. **92**, 137202 (2004).